

Rayleigh Scattering from a Sphere Located Near a Planar Rigid Boundary

Alexey Maksimov 

*Pacific Oceanological Institute
Far Eastern Branch of the Russian Academy of Sciences,
Vladivostok, 690041, Russia
maksimov@poi.dvo.ru*

Received 15 October 2023

Revised 21 January 2024

Accepted 22 January 2024

Published 3 April 2024

Rayleigh scattering from a spherical object located near a planar rigid boundary at distances smaller than the wavelength is calculated. Low frequency analysis reduces a scattering problem to a sequence of potential problems. An analytical solution based on expansion in spherical solid harmonics and the use of addition theorem is presented. Analytical perturbation approach is validated by comparison with numerical calculations. The velocity of the center of the particle and the scattering amplitude are determined. In the lowest order in wavenumber, the scattering amplitude is expressed in terms of the monopole and dipole components. In contrast to the behavior of a bubble, under the same conditions, dipole oscillations of the particle in the direction normal to the boundary are not excited and the monopole component of the scattering amplitude does not depend on the location of the particle relative to the boundary.

Keywords: Rayleigh scattering; fluid sphere; rigid boundary; particle velocity; scattering amplitude.

1. Introduction

The scattering of an acoustic wave by an object located near bounding interfaces has been a subject of active research for decades. The applications are diverse, including: underwater acoustics, acoustical oceanography, medical, and industrial ultrasound. In problems of underwater acoustics, the dimensions of the object usually exceed the spatial scale of the probing signal.^{1–5} At the same time, in applications that use acoustic methods for manipulating objects^{6,7} and ultrasonic cleaning,⁸ as a rule, the sizes of particles are small compared to the wavelength.

The scattering of an acoustic wave by an object whose dimensions are small in comparison with the wavelength is referred to as Rayleigh scattering.⁹ The presence of the bounding interface has a considerable effect on the way in which the particle scatters an incident field. To gain an understanding of how the object-interface interaction affects the scattering amplitude at low frequencies a number of different models are treated. The scattering of a plane

sound wave by a sphere near a hard or soft screen was investigated in Ref. 1,2. This problem was solved by introducing imaginary sources and was reduced to describing scattering by two spheres. The use of bispherical coordinates made it possible to obtain an analytical description of Rayleigh scattering by gas bubbles near the soft¹⁰ and rigid boundaries.¹¹ Special approaches are required to analyze the situation when the wavelength exceeds one of the dimensions of the object, but is small compared to other object sizes.¹²

If the screen is neither acoustically hard nor acoustically soft, the problem cannot be reduced to scattering by two spheres and other methods must be used. The solution can be obtained by applying the integral Helmholtz equation, in which the field of a point source in a half-space with an elastic boundary is used as the Green's function.³ The diffraction field is presented in the form of an expansion in spherical harmonics, and the coefficients of this expansion are determined as solutions of algebraic systems of equations. The possibility of finding an analytical solution to these equations was demonstrated in Refs. 13,14 for the limiting case of Rayleigh scattering by a gas bubble near an elastic boundary.

Acoustic radiation pressure offers a means of manipulating particles within a fluid. For Rayleigh scattering¹⁵ and low contrast particles,¹⁶ the radiation pressure can be described analytically. In recent years, there have been also analyses devoted specifically to the acoustic radiation force on a particle located near an interface.^{17–20} Approximate numerical solutions for the infinite linear system have been obtained by truncating the spherical wave expansion at a finite number in these studies.^{17,18,20} In addition, a finite element model was also employed.^{19,20}

The linear low-frequency scattering solution developed in the present work for a penetrable (fluid) sphere near a rigid boundary is based on the analysis pertaining to bubble^{11,13,14} and rigid sphere.²¹ The emphasis is on obtaining an approximate analytical description that allows one to give a physical interpretation of the results obtained and use analytical expressions in the analysis of nonlinear effects. Following Dassios,²² low frequency analysis is used to reduce a scattering problem to a sequence of potential problems. In the current study, more realistic (kinematic and dynamic) boundary conditions on the particle surface were used compared to the Dirichlet and Neumann conditions used in the Ref. 22. The method of the recursive relations derived by Doinikov²³ has been used for obtaining approximate solutions. Numerical calculations validate obtained analytical formulas. As applications of the obtained results, the oscillatory velocity of the particle center and the scattering amplitude are determined.

2. Formulation of the Problem

The incident wave, defined by the velocity potential φ_{in} , scatters on a penetrable (fluid) sphere with a surface S_p located in the upper half-space V_+ with an impenetrable lower boundary S_g ($z = 0$). The sphere radius R_p and the distance from the particle center to the boundary h are much smaller than the wavelength. The geometry of the problem is illustrated in Fig. 1.

Let us introduce notation for a point $\mathbf{r} = (x, y, z)$ and its mirror image $\mathbf{r}_i = (x, y, -z)$. Consider the function $\varphi_0(\mathbf{r})$ that describes the solution of the scattering problem in the

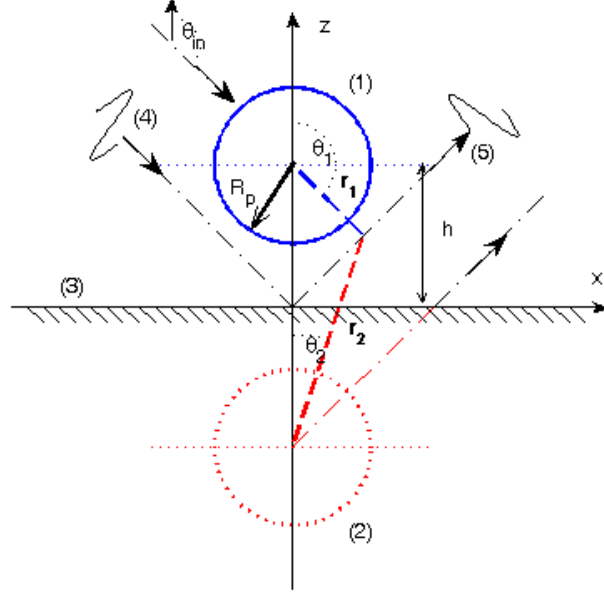


Fig. 1. Illustration of the geometry of the problem: an incident wave (4) propagates in the direction of the wave vector $\mathbf{k}/k = (\sin \theta_{in}, 0, \cos \theta_{in})$ and scatters on a particle of radius R_p (1) located at a distance h from the boundary of an impenetrable medium (3). The mirror particle (2) is used to describe the interaction with the boundary. Spherical coordinate systems centered on the particle $\mathbf{r}_1 = (r_1, \theta_1, \alpha)$ and its mirror image (2) $\mathbf{r}_2 = (r_2, \theta_2, \alpha)$, $\mathbf{r}_2 = \mathbf{r}_1 + 2h\mathbf{e}_z$ are used to construct a potential solution to the boundary value problem.

absence of the particle $\varphi_0(\mathbf{r}) = \varphi_{in}(\mathbf{r}) + \varphi_{in}(\mathbf{r}_i)$ (the incident (4) and reflected (5) waves in Fig. 1).

It is required to determine the scattered field φ^s in the upper half-space and the field inside the particle φ^{tr} , which satisfy the following equations and boundary conditions

$$\begin{aligned} \nabla^2 \varphi^s(\mathbf{r}) + k^2 \varphi^s(\mathbf{r}) &= 0, \quad \mathbf{r} \in V_+, \quad \varphi^T = \varphi_0 + \varphi^s, \\ (\mathbf{n} \cdot \nabla) \varphi^T &= (\mathbf{n} \cdot \nabla) \varphi^{tr}, \quad \varphi^s = (\rho_p / \rho_0) \varphi^{tr}, \quad \mathbf{r} \in S_p, \\ \nabla^2 \varphi^{tr}(\mathbf{r}) + k^2 \eta^2 \varphi^{tr}(\mathbf{r}) &= 0, \quad \mathbf{r} \in V_p, \quad (\mathbf{n}' \cdot \nabla) \varphi^s = 0, \quad \mathbf{r} \in S_g, \end{aligned} \quad (1)$$

here \mathbf{n} and \mathbf{n}' are the outward normals with respect to the particle and the lower medium, V_p is the volume of the particle, $\eta = c_0/c_p$, c_0 and c_p are the speeds of sound in the medium and the material of the particle, ρ_0 and ρ_p are the densities of the medium and the particle, φ^T is the total field.

The Helmholtz equation in the upper half-space can be written in the integral form

$$\varphi^s(\mathbf{r}) = \frac{1}{4\pi} \int_{S_p + S_g} \left\{ \varphi^s(\mathbf{r}') \frac{\partial G(\mathbf{r}, \mathbf{r}')}{\partial n'} - G(\mathbf{r}, \mathbf{r}') \frac{\partial \varphi^s(\mathbf{r}')}{\partial n'} \right\} dS', \quad (2)$$

where $G(\mathbf{r}, \mathbf{r}')$ is the Green's function. The choice of the Green's function satisfying the boundary condition on S_g ($z = 0$),

$$G(\mathbf{r}, \mathbf{r}') = \frac{e^{ikR}}{R} + \frac{e^{ikR_i}}{R_i}, \quad R = \sqrt{(x - x')^2 + (y - y')^2 + (z - z')^2}$$

$$R_i = \sqrt{(x - x')^2 + (y - y')^2 + (z + z')^2}, \quad (3)$$

leads to the fact that the integration in Eq.(2) is carried out only over the surface of the particle.

Since φ_0 also satisfies this integral equation, then for the total field $\varphi^T = \varphi_0 + \varphi^s$ we have:

$$\varphi^T(\mathbf{r}) = \varphi_0(\mathbf{r}) + \frac{1}{4\pi} \int_{S_p} \left\{ \varphi^T(\mathbf{r}') \frac{\partial}{\partial n'} \left[\frac{e^{ikR}}{R} + \frac{e^{ikR_i}}{R_i} \right] - \left[\frac{e^{ikR}}{R} + \frac{e^{ikR_i}}{R_i} \right] \frac{\partial \varphi^T(\mathbf{r}')}{\partial n'} \right\} dS'. \quad (4)$$

The integral representation for the field inside the particle is written as

$$\varphi^{tr}(\mathbf{r}) = \frac{1}{4\pi} \int_{S_p} \left\{ \varphi^{tr}(\mathbf{r}') \frac{\partial}{\partial n'} \left(\frac{e^{ik\eta R}}{R} \right) - \frac{e^{ik\eta R}}{R} \frac{\partial \varphi^{tr}(\mathbf{r}')}{\partial n'} \right\} dS'. \quad (5)$$

When finding a solution in the long-wavelength approximation, we will use the technique proposed in Ref. 22.

Let us represent the low-frequency expansion of the quantities included in the Eqs.(4-5) in the form:

$$\varphi_0(\mathbf{r}) = \sum_{n=0}^{\infty} \frac{(ikR_p)^n}{n!} \varphi_{0n}(\mathbf{r}), \quad \varphi^s(\mathbf{r}) = \sum_{n=0}^{\infty} \frac{(ikR_p)^n}{n!} \varphi_n^s(\mathbf{r}), \quad \varphi^{tr}(\mathbf{r}) = \sum_{n=0}^{\infty} \frac{(ikR_p)^n}{n!} \varphi_n^{tr}(\mathbf{r}). \quad (6)$$

If $\varphi_{in}(\mathbf{r})$ is a plane wave $\varphi_{in}(\mathbf{r}) = \varphi_m \exp[i(\mathbf{k} \cdot \mathbf{r}) - i\omega t]$ propagating in the direction $\mathbf{e}_k = \mathbf{k}/k$, then $\varphi_{0n}(\mathbf{r})/\varphi_m = [(\mathbf{e}_k \cdot \mathbf{r})/R_p]^n + [(\mathbf{e}_k \cdot \mathbf{r}_i)/R_p]^n$. In a spherical coordinate system associated with the center of the particle we have $\mathbf{e}_k = (\sin \theta_{in} \cos \alpha_{in}, \sin \theta_{in} \sin \alpha_{in}, \cos \theta_{in})$.

Substituting the expansion of the Green's function, we obtain equations for the required quantities

$$\varphi_n^T(\mathbf{r}) = \varphi_{0n}(\mathbf{r}) + \frac{1}{4\pi} \sum_{l=0}^n \binom{n}{l} \frac{1}{R_p^l} \int_{S_p} \left\{ \varphi_{n-l}^T(\mathbf{r}') \frac{\partial}{\partial n'} [R^{l-1} + R_i^{l-1}] \right.$$

$$\left. - [R^{l-1} + R_i^{l-1}] \frac{\partial \varphi_{n-l}^T(\mathbf{r}')}{\partial n'} \right\} dS'. \quad (7)$$

This equation expresses the n th expansion term in terms of all the previous ones, including the n th one. However, the advantage of this notation is that the term containing on the right side $\varphi_n^T(\mathbf{r}')$, $\partial \varphi_n^T(\mathbf{r}')/\partial n'$ is a potential function – the solution of the Laplace equation.²²

Therefore, the desired solution can be represented as

$$\begin{aligned}
 \varphi_n^T(\mathbf{r}) &= F_n(\mathbf{r}) + \phi_n(\mathbf{r}), \\
 F_n(\mathbf{r}) &= \varphi_{0n}(\mathbf{r}) + \frac{1}{4\pi} \sum_{l=1}^n \binom{n}{l} \frac{1}{R_p^l} \int_{S_p} \left\{ \varphi_{n-l}^T(\mathbf{r}') \frac{\partial}{\partial n'} [R^{l-1} + R_i^{l-1}] \right. \\
 &\quad \left. - [R^{l-1} + R_i^{l-1}] \frac{\partial \varphi_{n-l}^T(\mathbf{r}')}{\partial n'} \right\} dS', \\
 \phi_n(\mathbf{r}) &= \frac{1}{4\pi} \frac{1}{R_p^l} \int_{S_p} \left\{ \varphi_n^T(\mathbf{r}') \frac{\partial}{\partial n'} [R^{-1} + R_i^{-1}] - [R^{-1} + R_i^{-1}] \frac{\partial \varphi_n^T(\mathbf{r}')}{\partial n'} \right\} dS'. \quad (8)
 \end{aligned}$$

For the solution inside the particle, we have:

$$\begin{aligned}
 \varphi_n^{tr}(\mathbf{r}) &= F_n^{tr}(\mathbf{r}) + \phi_n^{tr}(\mathbf{r}), \\
 F_n^{tr}(\mathbf{r}) &= \frac{1}{4\pi} \sum_{l=1}^n \binom{n}{l} \frac{\eta^l}{R_p^l} \int_{S_p} \left\{ \varphi_{n-l}^{tr}(\mathbf{r}') \frac{\partial R^{l-1}}{\partial n'} - R^{l-1} \frac{\partial \varphi_{n-l}^{tr}(\mathbf{r}')}{\partial n'} \right\} dS', \\
 \phi_n^{tr}(\mathbf{r}) &= \frac{1}{4\pi} \frac{\eta^l}{R_p^l} \int_{S_p} \left\{ \varphi_n^{tr}(\mathbf{r}') \frac{\partial}{\partial n'} R^{-1} - R^{-1} \frac{\partial \varphi_n^{tr}(\mathbf{r}')}{\partial n'} \right\} dS'. \quad (9)
 \end{aligned}$$

Thus, if we know $\varphi_m^T(\mathbf{r})$ for $m = 0, 1, \dots, (n-1)$, then finding it is reduced to solving the following boundary value problem for $\phi_n(\mathbf{r})$ and $\phi_n^{tr}(\mathbf{r})$:

$$\begin{aligned}
 \nabla^2 \phi_n(\mathbf{r}) &= 0, \quad \mathbf{r} \in V_+, \quad \nabla^2 \phi_n^{tr}(\mathbf{r}) = 0, \quad \mathbf{r} \in V_p, \quad \frac{\partial \phi_n}{\partial n'} = 0, \quad \mathbf{r}' \in S_g, \\
 \frac{\partial(\phi_n + F_n)}{\partial n'} &= \frac{\partial(\phi_n^{tr} + F_n^{tr})}{\partial n'}, \quad F_n(\mathbf{r}) + \phi_n(\mathbf{r}) = (\rho_p/\rho_0) [F_n^{tr}(\mathbf{r}) + \phi_n^{tr}(\mathbf{r})], \quad \mathbf{r} \in S_p. \quad (10)
 \end{aligned}$$

The first expansion terms have the following form:

$$\begin{aligned}
 F_0 &= \varphi_0 = 2\varphi_m, \quad \phi_0(\mathbf{r}) = 0, \quad \varphi_0^T(\mathbf{r}) = F_0 + \phi_0 = 2\varphi_m, \quad F_0^{tr} = 0, \quad \phi_0^{tr} = (\rho_0/\rho_p) 2\varphi_m, \\
 F_1 &= \varphi_{01} = 2\varphi_m [\sin \theta \sin \theta_{in} \cos(\alpha - \alpha_{in})(r/R_p) + \cos \theta_{in}(h/R_p)], \quad F_1^{tr} = 0. \quad (11)
 \end{aligned}$$

The description of Rayleigh scattering by a penetrating particle located near the interface reduces in the lowest order to solving the boundary value problem (10) with the following form of boundary conditions on the particle surface:

$$\begin{aligned}
 \frac{\partial \phi_1}{\partial r} \Big|_{r=R_p} + 2 \left(\frac{\varphi_m}{R_p} \right) \sin \theta \sin \theta_{in} \cos(\alpha - \alpha_{in}) &= \frac{\partial \phi_1^{tr}}{\partial r} \Big|_{r=R_p}, \\
 \phi_1(R_p) + 2\varphi_m \sin \theta \sin \theta_{in} \cos(\alpha - \alpha_{in}) &= (\rho_p/\rho_0) \phi_1^{tr}(R_p). \quad (12)
 \end{aligned}$$

The direction of the x -axis can be chosen along the projection of the wave vector, so that $\alpha_{in} = 0$.

3. Computation of the First order Solution

Following Doinikov,²³ we are looking for a solution (outside the particle) in the form of a sum of potentials centered on the particle and its mirror image

$$\phi_1 = \sum_{l=0}^{\infty} \sum_{m=-l}^l \left[a_{lm} R_p^{l+1} I_{lm}(\mathbf{r}_1) + b_{lm} R_p^{l+1} I_{lm}(\mathbf{r}_2) \right], \quad I_{lm}(\mathbf{r}) = \sqrt{\frac{4\pi}{2l+1}} \frac{Y_{lm}(\theta, \alpha)}{r^{l+1}}, \quad (13)$$

here Y_{lm} are spherical functions, I_{lm} are irregular solid harmonics,²⁴ $\mathbf{r}_2 = \mathbf{r}_1 + 2h\mathbf{e}_z$. In order to satisfy the boundary conditions at $z = 0$, it is necessary to fulfill the conditions $b_{lm} = (-1)^{l+m} a_{lm}$.

To fulfill the boundary conditions on the surface of the particle, it is necessary to transform the spatial harmonics centered on the mirror image to the coordinates centered on the particle. The addition theorems²⁵ provide this connection.

$$I_{lm}(\mathbf{r}_1 + 2h\mathbf{e}_z) = \sum_{\lambda=|m|}^{\infty} (-1)^{\lambda+m} \sqrt{\frac{4\pi}{2\lambda+1}} \sqrt{\frac{(l+\lambda)!(l+\lambda)!}{(l+m)!(l-m)!(\lambda+m)!(\lambda-m)!}} \frac{r^\lambda Y_{lm}(\theta, \alpha)}{2h^{\lambda+l+1}}. \quad (14)$$

The potential of the first approximation for the field outside the particle then takes the form

$$\begin{aligned} \phi_1 = & \sum_{l=0}^{\infty} \sum_{m=-l}^l a_{lm} \left[\left(\frac{R_p}{r_1} \right)^{l+1} Y_{lm}(\theta_1, \alpha) + \sum_{\lambda=|m|}^{\infty} (-1)^{\lambda+m} \sqrt{\frac{2l+1}{2\lambda+1}} \right. \\ & \times \left. \sqrt{\frac{(l+\lambda)!(l+\lambda)!}{(l+m)!(l-m)!(\lambda+m)!(\lambda-m)!}} \frac{r^\lambda R_p^{l+1}}{(2h)^{\lambda+l+1}} Y_{\lambda m}(\theta_1, \alpha) \right], \end{aligned} \quad (15)$$

where we have kept the notation a_{lm} for the renormalized expansion coefficients $a_{lm} \sqrt{4\pi/(2l+1)} \rightarrow a_{lm}$

The potential of the first approximation inside the particle is described by the following expression:

$$\phi_1^{tr} = \sum_{l=0}^{\infty} \sum_{m=-l}^l c_{lm} \left(\frac{r_1}{R_p} \right)^l Y_{lm}(\theta_1, \alpha). \quad (16)$$

Substituting (15) and (16) into boundary conditions (12) and projecting onto Y_{LM}^* gives

$$\begin{aligned} a_{LM} - \frac{L(\rho_p - \rho_0)}{(L+1)\rho_p + L\rho_0} \sum_{l=|M|}^{\infty} a_{lM} (-1)^{l+L} \sqrt{\frac{2l+1}{2L+1}} \sqrt{\frac{(l+L)!(l+L)!}{(l+m)!(l-m)!(L+m)!(L-m)!}} \\ \times \left(\frac{R_p}{2h} \right)^{L+l+1} = -2\varphi_m \sqrt{\frac{2\pi}{3}} \frac{(\rho_p - \rho_0)}{2\rho_p + \rho_0} \sin \theta_{in} \delta_{L1} (\delta_{M1} - \delta_{M-1}), \end{aligned} \quad (17)$$

The form of the right-hand side of (17) determines the presence of only the following components $M = \pm 1$.

The power-law dependence of the coefficients on the parameter $\epsilon = (R_p/2h)$ makes it possible, following Doinikov,²³ to seek a solution in the form

$$\begin{aligned}
 a_{LM} &= \varphi_0 \sqrt{\frac{2\pi}{3}} \frac{(\rho_p - \rho_0)}{2\rho_p + \rho_0} \sin \theta_{in} \left(\frac{R_p}{2h} \right)^{L-1} \sum_{k=0}^{\infty} \alpha_{Lk}^{(1)} \left(\frac{R_p}{2h} \right)^k, \quad M = 1, \\
 \sum_{k=0}^{\infty} \alpha_{Lk}^{(1)} \left(\frac{R_p}{2h} \right)^k &- \frac{L(\rho_p - \rho_0)}{(L+1)\rho_p + L\rho_0} \sum_{l=1}^{\infty} (-1)^{l+L} \sqrt{\frac{2l+1}{2L+1}} \\
 &\times \sqrt{\frac{(l+L)!(l+L)!}{(l+1)!(l-1)!(L+1)!(L-1)!}} \sum_{m=0}^{\infty} \alpha_{lk}^{(1)} \left(\frac{R_p}{2h} \right)^{2l+m+1} = -\delta_{L1}. \quad (18)
 \end{aligned}$$

Equating the coefficients at the same powers ϵ , we get:

$$\begin{aligned}
 \alpha_{Lk}^{(1)} \left(\frac{R_p}{2h} \right)^k &- \frac{L(\rho_p - \rho_0)}{(L+1)\rho_p + L\rho_0} \sum_{l=1}^{\infty} (-1)^{l+L} \sqrt{\frac{2l+1}{2L+1}} \\
 &\times \sqrt{\frac{(l+L)!(l+L)!}{(l+1)!(l-1)!(L+1)!(L-1)!}} \alpha_{l(k-2l-1)}^{(1)} = -\delta_{L1} \delta_{k0}. \quad (19)
 \end{aligned}$$

As noted in Ref. 23, the resulting relations are, in essence, recursive formulas that allow one to find the solution in an explicit form:

$$\begin{aligned}
 \alpha_{10}^{(1)} &= -1, \alpha_{L0}^{(1)} = 0, (L = 2, 3, \dots), \alpha_{L1}^{(1)} = 0, \alpha_{L2}^{(1)} = 0, \alpha_{0k}^{(1)} = 0, (k = 0, 1, 2, 3, \dots), \\
 \alpha_{L3}^{(1)} &= \frac{L(\rho_p - \rho_0)}{(L+1)\rho_p + L\rho_0} \sum_{l=1}^{\infty} (-1)^{l+L} \sqrt{\frac{2l+1}{2L+1}} \sqrt{\frac{(l+L)!(l+L)!}{(l+1)!(l-1)!(L+1)!(L-1)!}} \alpha_{l(3-2l-1)}^{(1)} \\
 &= \frac{L(\rho_p - \rho_0)}{(L+1)\rho_p + L\rho_0} (-1)^{1+L} \sqrt{\frac{3}{2L+1}} \sqrt{\frac{(1+L)!}{2(L-1)!}} \alpha_{10}^{(1)} \\
 &= \frac{L(\rho_p - \rho_0)}{(L+1)\rho_p + L\rho_0} (-1)^L \sqrt{\frac{3}{2L+1}} \sqrt{\frac{(1+L)!}{2(L-1)!}}, \\
 \alpha_{13}^{(1)} &= -\frac{(\rho_p - \rho_0)}{2\rho_p + \rho_0}, \alpha_{23}^{(1)} = \frac{6}{\sqrt{5}} \frac{(\rho_p - \rho_0)}{3\rho_p + 2\rho_0}, \alpha_{33}^{(1)} = -9 \sqrt{\frac{2}{7}} \frac{(\rho_p - \rho_0)}{4\rho_p + 3\rho_0}, \\
 \alpha_{43}^{(1)} &= 4 \sqrt{\frac{2 \cdot 5}{3}} \frac{(\rho_p - \rho_0)}{5\rho_p + 4\rho_0}, \alpha_{53}^{(1)} = -15 \sqrt{\frac{5}{11}} \frac{(\rho_p - \rho_0)}{6\rho_p + 5\rho_0}, \\
 \alpha_{L6}^{(1)} &= \frac{L(\rho_p - \rho_0)}{(L+1)\rho_p + L\rho_0} \sum_{l=1}^{\infty} (-1)^{l+L} \sqrt{\frac{2l+1}{2L+1}} \sqrt{\frac{(l+L)!(l+L)!}{(l+1)!(l-1)!(L+1)!(L-1)!}} \alpha_{l(6-2l-1)}^{(1)} \\
 &= (-1)^{1+L} \frac{L(\rho_p - \rho_0)}{(L+1)\rho_p + L\rho_0} \sqrt{\frac{3}{2L+1}} \sqrt{\frac{(1+L)!}{2(L-1)!}} \alpha_{13}^{(1)} = -\alpha_{L3}^{(1)} \alpha_{13}^{(1)}, \\
 \alpha_{L7}^{(1)} &= 0. \quad (20)
 \end{aligned}$$

The accuracy of the representation of the solution is determined by the degree of the parameter $\epsilon = (R_p/2h) < 1/2$, so two orders of magnitude accuracy is ensured by taking into account the terms up to $\epsilon^7 \approx 0.01$. With this accuracy, the solution has the form:

$$\begin{aligned}
\phi_1 &= \sum_{l=1}^5 a_{l1} \left\{ \left(\frac{R_p}{r_1} \right)^{l+1} [Y_{l1}(\theta_1, \alpha) + Y_{l1}^*(\theta_1, \alpha)] + (-1)^{l+1} \left(\frac{R_p}{r_2} \right)^{l+1} [Y_{l1}(\theta_2, \alpha) + Y_{l1}^*(\theta_2, \alpha)] \right\}, \\
a_{11} &= \sqrt{\frac{2\pi}{3}} \varphi_0 \frac{(\rho_p - \rho_0)}{(2\rho_p + \rho_0)} \sin \theta_{in} \left[\alpha_{10}^{(1)} + \alpha_{13}^{(1)} \left(\frac{R_p}{2h} \right)^3 + \alpha_{16}^{(1)} \left(\frac{R_p}{2h} \right)^6 \right] \\
&= -\sqrt{\frac{2\pi}{3}} \varphi_0 \frac{(\rho_p - \rho_0)}{(2\rho_p + \rho_0)} \sin \theta_{in} \left[1 + \frac{(\rho_p - \rho_0)}{(2\rho_p + \rho_0)} \left(\frac{R_p}{2h} \right)^3 + \frac{(\rho_p - \rho_0)^2}{(2\rho_p + \rho_0)^2} \left(\frac{R_p}{2h} \right)^6 \right], \\
a_{21} &= \sqrt{\frac{2\pi}{3}} \varphi_0 \frac{(\rho_p - \rho_0)}{2\rho_p + \rho_0} \sin \theta_{in} \left[\alpha_{23}^{(1)} \left(\frac{R_p}{2h} \right)^4 + \alpha_{26}^{(1)} \left(\frac{R_p}{2h} \right)^7 \right] \\
&= \sqrt{\frac{2\pi}{3 \cdot 5}} 6\varphi_0 \frac{(\rho_p - \rho_0)}{2\rho_p + \rho_0} \sin \theta_{in} \left[\frac{(\rho_p - \rho_0)}{(3\rho_p + 2\rho_0)} \left(\frac{R_p}{2h} \right)^4 + \frac{(\rho_p - \rho_0)^2}{(2\rho_p + \rho_0)(3\rho_p + 2\rho_0)} \left(\frac{R_p}{2h} \right)^7 \right], \\
a_{31} &= \sqrt{\frac{2\pi}{3}} \varphi_0 \frac{(\rho_p - \rho_0)}{(2\rho_p + \rho_0)} \sin \theta_{in} \alpha_{33}^{(1)} \left(\frac{R_p}{2h} \right)^5 = \sqrt{\frac{4\pi}{3 \cdot 7}} 9\varphi_0 \sin \theta_{in} \\
&\quad \times \frac{(\rho_p - \rho_0)^2}{(2\rho_p + \rho_0)(4\rho_p + 3\rho_0)} \left(\frac{R_p}{2h} \right)^5, \\
a_{41} &= \sqrt{\frac{2\pi}{3}} \varphi_0 \frac{(\rho_p - \rho_0)}{(2\rho_p + \rho_0)} \sin \theta_{in} \alpha_{43}^{(1)} \left(\frac{R_p}{2h} \right)^6 = \sqrt{5\pi} \frac{8}{3} \varphi_0 \sin \theta_{in} \\
&\quad \frac{(\rho_p - \rho_0)^2}{(2\rho_p + \rho_0)(5\rho_p + 4\rho_0)} \left(\frac{R_p}{2h} \right)^6, \\
a_{51} &= \sqrt{\frac{2\pi}{3}} \varphi_0 \frac{(\rho_p - \rho_0)}{(2\rho_p + \rho_0)} \sin \theta_{in} \alpha_{53}^{(1)} \left(\frac{R_p}{2h} \right)^7 = \sqrt{\frac{2\pi \cdot 5}{11}} 15\varphi_0 \sin \theta_{in} \\
&\quad \frac{(\rho_p - \rho_0)^2}{(2\rho_p + \rho_0)(6\rho_p + 5\rho_0)} \left(\frac{R_p}{2h} \right)^7. \quad (21)
\end{aligned}$$

When deriving Eq.(21), we used the fact that $a_{l-1} = -a_{l1}$ and $Y_{l-1} = -Y_{l1}^*$.

An approximate numerical solution for the infinite system (17) is obtained by truncating the spherical harmonic expansion at a finite number N such that $L = 1, \dots, N$. As noted in Ref. 20, when carrying out similar calculations, the method used turns out to be effective. Thus, at $N = 10$, the accuracy exceeds 10^{-3} . We present a solution for a_{L1} only, since a_{L-1} is simply related to a_{L1} : $a_{L-1} = -a_{L1}$. Moreover, in order to make it convenient to compare with the results of analytical consideration, numerical calculations are performed for normalized values A_L : $a_{L1} = \varphi_0 \sqrt{\frac{2\pi}{3}} \frac{(\rho_p - \rho_0)}{2\rho_p + \rho_0} \sin \theta_{in} A_L$.

Figure 2(a,b) illustrates the dependence of the normalized amplitudes as a function of the distance from the particle center to the boundary h/R_p for the first two modes

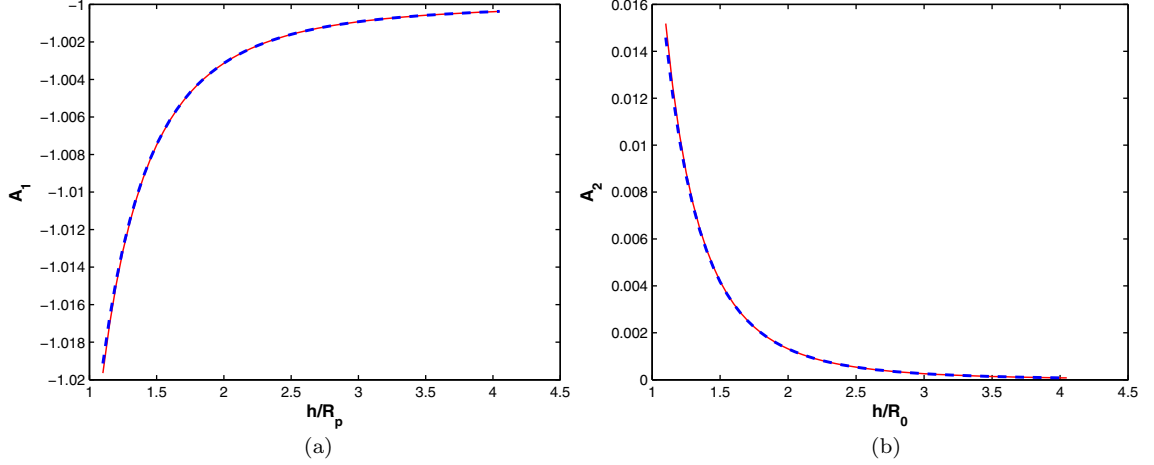


Fig. 2. The variations in the normalized amplitude of the first A_1 and the second A_2 modes with the dimensionless distance h/R_p are shown in panel (a) and (b), correspondingly. Numerical calculations are indicated by the solid lines. The dashed lines show the contribution of the analytical approach given by (17).

$L = 1, 2$. Namely, for these modes, the influence of the boundary is most significant. The smallness of the values of the relative amplitudes of the nondominant modes complicates their graphical representation. The results, presented in Fig. 2(a,b), have been obtained for typical parameters of media²⁰ ($\rho_p/\rho_0 = 2$).

Comparison of the plots presented in Fig. 2(a,b) shows that the perturbation (analytical) approach quite satisfactory conveys the behavior of the amplitudes, in particular, their variation with the distance.

We ignore the effect of the viscosity, assuming that the thickness of the viscous layer is small compared to the particle radius. However, near the boundary, this condition should be tightened, and the gap between the particle wall and the boundary should be greater than the thickness of the boundary layer. To avoid violating these constraints, we performed numerical calculations under the condition that the size of the gap exceeds one-tenth of the particle radius.

4. Vibrational Velocity of a Particle

The velocity of the particle center is determined from the condition of the balance of inertial forces and pressure acting on the surface of the particle, which, in the approximation linear in the wavenumber, reduces to

$$\rho_p \frac{4\pi R_p^3}{3} \frac{d\mathbf{u}}{dt} = - \int_{S_p} p \mathbf{n}' dS', \quad \rho_p \frac{4\pi R_p^3}{3} \mathbf{u} = \rho_0 (ikR_p) \int_{S_p} (F_1(\mathbf{r}') + \phi_1(\mathbf{r}')) \mathbf{n}' dS'. \quad (22)$$

The calculation of the surface integral leads to the following expressions:

$$\begin{aligned}
\rho_p \frac{4\pi R_p^3}{3} u_x &= \rho_0(ik) R_p^3 \int_0^\pi \int_0^{2\pi} \sin \theta' d\theta' d\alpha' (F_1(\theta', \alpha') + \phi_1(\theta', \alpha')) \sin \theta' \cos \alpha', \\
\rho_0(ik) R_p^3 \int_0^\pi \int_0^{2\pi} \sin \theta' d\theta' d\alpha' F_1(\theta', \alpha') \sin \theta' \cos \alpha' &= \rho_0 \frac{4\pi R_p^3}{3} (ik) \varphi_0 \sin \theta_{in}, \\
\rho_0(ik) R_p^3 \int_0^\pi \int_0^{2\pi} \sin \theta' d\theta' d\alpha' \phi_1(\theta', \alpha') &= -\rho_0(ik) R_p^3 \sqrt{\frac{8\pi}{3}} \left\{ a_{11} \left[1 + \left(\frac{R_p}{2h} \right)^3 \right] \right. \\
&+ \sum_{l=2}^{\infty} (-1)^{l+1} \sqrt{\frac{2l+1}{3}} \sqrt{\frac{(l+1)!}{2(l-1)!}} \left(\frac{R_p}{2h} \right)^{l+2} \left. \right\} \approx -\rho_0(ik) R_p^3 \sqrt{\frac{8\pi}{3}} a_{11} \left[1 + \left(\frac{R_p}{2h} \right)^3 \right] \\
&\approx \frac{4\pi R_p^3}{3} \rho_0(ik) \varphi_0 \sin \theta_{in} \left[\frac{(\rho_p - \rho_0)}{(2\rho_p + \rho_0)} + \frac{3\rho_p(\rho_p - \rho_0)}{(2\rho_p + \rho_0)^2} \left(\frac{R_p}{2h} \right)^3 \right. \\
&\quad \left. + \frac{3\rho_p(\rho_p - \rho_0)^2}{(2\rho_p + \rho_0)^3} \left(\frac{R_p}{2h} \right)^6 \right], \\
u_x &= v_x^{(0)} \left[\frac{3\rho_p}{(2\rho_p + \rho_0)} + \frac{3\rho_p(\rho_p - \rho_0)}{(2\rho_p + \rho_0)^2} \left(\frac{R_p}{2h} \right)^3 + \frac{3\rho_p(\rho_p - \rho_0)^2}{(2\rho_p + \rho_0)^3} \left(\frac{R_p}{2h} \right)^6 \right], \quad (23)
\end{aligned}$$

where we introduced the notation $v_x^{(0)} = i\varphi_0 k \sin \theta_{in}$ for the velocity induced by the incident and reflected from the interface waves at a point coinciding with the center of the particle, but in the absence of the particle itself. As the distance to the boundary increases, the expression for the velocity turns into the well-known formula for a free particle.

5. Scattering Amplitude

It is convenient to describe the behavior of the scattered field in the far field $kr \gg 1$ in terms of the scattering amplitude: $\varphi^s/\varphi_0 \approx f(\theta, \alpha) (e^{ikr}/r)$. Using the representation for the scattered field Eq.(2) and the asymptotic for the Green's function, we obtain

$$\begin{aligned}
f(\theta, \alpha) &= \frac{1}{4\pi\varphi_0} \int_{S_p} \left\{ \varphi^T(\mathbf{r}') \frac{\partial}{\partial n'} \left[e^{-ik(\mathbf{e}_r \cdot \mathbf{r}') + e^{-ik(\mathbf{e}_r \cdot \mathbf{r}'_i)} \right] \right. \\
&\quad \left. - \left[e^{-ik(\mathbf{e}_r \cdot \mathbf{r}') + e^{-ik(\mathbf{e}_r \cdot \mathbf{r}'_i)} \right] \frac{\partial \varphi^T(\mathbf{r}')}{\partial n'} \right\} dS'. \quad (24)
\end{aligned}$$

Substituting into this expression the low-frequency expansion for the potential (6) and the components of the Green's function, we obtain

$$f(\theta, \alpha) = \sum_{l=0}^{\infty} \frac{(ikR_p)^l}{l!} \sum_{m=0}^l \frac{l!}{(l-m)!m!} \frac{(-1)^m}{4\pi\varphi_0} \int_{S_p} \left\{ -[(\mathbf{e}_r \cdot \mathbf{r}'/R_p)^m + (\mathbf{e}_r \cdot \mathbf{r}'_i/R_p)^m] \right. \\ \times \frac{\partial}{\partial n'} [F_{l-m}(\mathbf{r}') + \phi_{l-m}(\mathbf{r}')] + \frac{\partial}{\partial n'} [(\mathbf{e}_r \cdot \mathbf{r}'/R_p)^m + (\mathbf{e}_r \cdot \mathbf{r}'_i/R_p)^m] \\ \left. \times [F_{l-m}(\mathbf{r}') + \phi_{l-m}(\mathbf{r}')] \right\} dS'. \quad (25)$$

The first terms of the expansion $l = 0, m = 0$, $l = 1, m = 0, 1$ don't contribute. For terms of the second order ($l = 2$), we have:

$$f_2(\theta, \alpha) = -\frac{(kR_p)^2}{4\pi\varphi_0} \int_{S_p} \left\{ [(\mathbf{e}_r \cdot \mathbf{r}'/R_p) + (\mathbf{e}_r \cdot \mathbf{r}'_i/R_p)] \frac{\partial}{\partial n'} [F_1(\mathbf{r}') + \phi_1(\mathbf{r}')] \right. \\ + \frac{\partial}{\partial n'} [(\mathbf{e}_r \cdot \mathbf{r}'/R_p) + (\mathbf{e}_r \cdot \mathbf{r}'_i/R_p)] [F_1(\mathbf{r}') + \phi_1(\mathbf{r}')] \\ \left. + \frac{1}{2} \frac{\partial}{\partial n'} [(\mathbf{e}_r \cdot \mathbf{r}'/R_p)^2 + (\mathbf{e}_r \cdot \mathbf{r}'_i/R_p)^2] F_0(\mathbf{r}') \right\} dS'. \quad (26)$$

The calculation of the individual terms included in this expression leads to the following results:

$$f_2^{(1)}(\theta, \alpha) = -\frac{(kR_p)^2}{4\pi\varphi_0} \int_{S_p} \frac{1}{2} \frac{\partial}{\partial n'} [(\mathbf{e}_r \cdot \mathbf{r}'/R_p)^2 + (\mathbf{e}_r \cdot \mathbf{r}'_i/R_p)^2] F_0(\mathbf{r}') dS' = -\frac{2}{3} k^2 R_p^3. \quad (27)$$

This term is related to the monopole source at the center of the particle, which takes into account the compressibility of the medium surrounding the particle (in the second order in terms of the wave number) caused by the incident field.

Calculation of the term associated with the vibrational velocity of the particle,

$$f_2^{(2)}(\theta, \alpha) = -\frac{(kR_p)^2}{4\pi\varphi_0} \int_{S_p} [(\mathbf{e}_r \cdot \mathbf{r}'/R_p) + (\mathbf{e}_r \cdot \mathbf{r}'_i/R_p)] \frac{\partial}{\partial n'} [F_1(\mathbf{r}') + \phi_1(\mathbf{r}')] , \quad (28)$$

is divided into two stages: finding the contribution induced by the incident field

$$f_2^{(2a)}(\theta, \alpha) = -\frac{k^2 R_p^4}{4\pi\varphi_0} \int_0^\pi \int_0^{2\pi} \sin \theta' d\theta' d\alpha' [2(\mathbf{e}_r \cdot \mathbf{n}'/R_p) - (2h/R_p)(\mathbf{e}_r \cdot \mathbf{e}_z)] \frac{\partial F_1(\mathbf{r}')}{\partial n'} \\ = -\frac{k^2 R_p^4}{4\pi\varphi_0} \int_0^\pi \int_0^{2\pi} \sin \theta' d\theta' d\alpha' [2(\mathbf{e}_r \cdot \mathbf{n}') - (2h/R_p)(\mathbf{e}_r \cdot \mathbf{e}_z)] \frac{\varphi_0}{R_p} \sin \theta_{in} \sin \theta' \cos \alpha' \\ = -\frac{2}{3} k^2 R_p^3 (\mathbf{e}_r \cdot \mathbf{e}_{\mathbf{k}_\perp}). \quad (29)$$

and the contribution induced by the scattered field:

$$f_2^{(2b)}(\theta, \alpha) = -\frac{k^2 R_p^4}{4\pi\varphi_0} \int_0^\pi \int_0^{2\pi} \sin \theta' d\theta' d\alpha' [2(\mathbf{e}_r \cdot \mathbf{n}'/R_p) - (2h/R_p)(\mathbf{e}_r \cdot \mathbf{e}_z)] \frac{\partial \phi_1(\mathbf{r}')}{\partial n'}$$

$$\begin{aligned}
&= -\frac{k^2 R_p^4}{4\pi\varphi_0} \int_0^\pi \int_0^{2\pi} \sin\theta' d\theta' d\alpha' 2 \sin\theta \sin\theta' \cos(\alpha - \alpha') 2 \sum_{l=0}^\infty a_{l1} \left[(-)(l+1) Y_{l1}(\theta', \alpha') \right. \\
&\quad \left. + \sum_{\lambda=1}^\infty (-1)^{\lambda+l} \lambda \sqrt{\frac{2l+1}{2\lambda+1}} \sqrt{\frac{(l+\lambda)!(l+\lambda)!}{(l+1)!(l-1)!(\lambda+1)!(\lambda-1)!}} \left(\frac{R_p}{2h}\right)^{l+\lambda+1} Y_{\lambda 1}(\theta', \alpha') \right] \\
&= -\frac{k^2 R_p^3}{4\pi\varphi_0} 8 \sqrt{\frac{2\pi}{3}} \sin\theta \cos\alpha \left[a_{11} - \frac{1}{2} \sum_{l=1}^\infty a_{l1} (-1)^{1+l} \sqrt{\frac{2l+1}{3}} \sqrt{\frac{(l+1)!}{2!(l-1)!}} \left(\frac{R_p}{2h}\right)^{l+2} \right] \\
&\quad \approx -\frac{k^2 R_p^3}{\sqrt{4\pi}\varphi_0} 4 \sqrt{\frac{2\pi}{3}} \sin\theta \cos\alpha a_{11} \left[1 - \frac{1}{2} \left(\frac{R_p}{2h}\right)^3 \right] \\
&\approx \frac{4}{3} k^2 R_p^3 (\mathbf{e}_r \cdot \mathbf{e}_{k_\perp}) \frac{(\rho_p - \rho_0)}{(2\rho_p + \rho_0)} \left[1 - \frac{3\rho_0}{2(2\rho_p + \rho_0)} \left(\frac{R_p}{2h}\right)^3 - \frac{3\rho_0(\rho_p - \rho_0)}{2(2\rho_p + \rho_0)^2} \left(\frac{R_p}{2h}\right)^6 \right], \quad (30)
\end{aligned}$$

here $\mathbf{e}_{k_\perp} = \mathbf{k}_\perp/k = (\sin\theta_{in}, 0, 0)$.

The calculation of the last term in Eq.(26), related to the potential distribution over the particle surface, will also be divided into two parts. First we find the contribution induced by the external field

$$\begin{aligned}
f_2^{(3a)}(\theta, \alpha) &= \frac{(kR_p)^2}{4\pi\varphi_0} \int_{S_p} \frac{\partial}{\partial n'} [(e_r \cdot \mathbf{r}'/R_p) + (e_r \cdot \mathbf{r}'_i/R_p)] F_1(\mathbf{r}') dS' \\
&= \frac{k^2 R_p^3}{4\pi} \int_0^\pi \int_0^{2\pi} \sin\theta' d\theta' d\alpha' 2 (e_r \cdot \mathbf{n}') \sin\theta_{in} \sin\theta' \cos\alpha' = \frac{2}{3} k^2 R_p^3 (e_r \cdot \mathbf{e}_{k_\perp}). \quad (31)
\end{aligned}$$

This term is related to the dipole source at the center of the particle, which takes into account the oscillatory displacements of the medium caused by the incident wave.

The calculation of the contribution associated with the scattered field is the most cumbersome:

$$\begin{aligned}
f_2^{(3b)}(\theta, \alpha) &= \frac{(kR_p)^2}{4\pi\varphi_0} \int_{S_p} \frac{\partial}{\partial n'} [(e_r \cdot \mathbf{r}'/R_p) + (e_r \cdot \mathbf{r}'_i/R_p)] \phi_1(\mathbf{r}') dS' \\
&= \frac{k^2 R_p^3}{4\pi} \int_0^\pi \int_0^{2\pi} \sin\theta' d\theta' d\alpha' 2 [\sin\theta \sin\theta' \cos(\alpha - \alpha') + \cos\theta \cos\theta'] \\
&\quad \left\{ \sum_{l=0}^\infty a_{l1} \left[Y_{l1}(\theta', \alpha') + \sum_{\lambda=1}^\infty (-1)^{\lambda+l} \sqrt{\frac{2l+1}{2\lambda+1}} \sqrt{\frac{(l+\lambda)!(l+\lambda)!}{(l+1)!(l-1)!(\lambda+1)!(\lambda-1)!}} \right. \right. \\
&\quad \left. \left. \times \left(\frac{R_p}{2h}\right)^{l+\lambda+1} Y_{\lambda 1}(\theta', \alpha') \right] \right. \\
&\quad \left. + \sum_{l=0}^\infty a_{l-1} \left[Y_{l-1}(\theta', \alpha') + \sum_{\lambda=1}^\infty (-1)^{\lambda+l} \sqrt{\frac{2l+1}{2\lambda+1}} \sqrt{\frac{(l+\lambda)!(l+\lambda)!}{(l+1)!(l-1)!(\lambda+1)!(\lambda-1)!}} \right. \right. \\
&\quad \left. \left. \times \left(\frac{R_p}{2h}\right)^{l+\lambda+1} Y_{\lambda-1}(\theta', \alpha') \right] \right\}
\end{aligned}$$

$$\begin{aligned}
 &= -k^2 R_p^3 \frac{2}{\sqrt{4\pi}\varphi_0} \sqrt{\frac{2}{3}} \sin \theta \cos \alpha \left[a_{11} + \sum_{l=1}^{\infty} a_{l1} (-1)^{1+l} \sqrt{\frac{2l+1}{3}} \sqrt{\frac{(l+1)!}{2!(l-1)!}} \left(\frac{R_p}{2h} \right)^{l+2} \right] \\
 &\approx -k^2 R_p^3 \frac{2}{\sqrt{4\pi}\varphi_0} \sqrt{\frac{2}{3}} \sin \theta \cos \alpha a_{11} \left[1 + \left(\frac{R_p}{2h} \right)^3 \right] \approx k^2 R_p^3 \frac{2}{\sqrt{4\pi}} \sqrt{\frac{2}{3}} \sin \theta \cos \alpha \sqrt{\frac{2\pi}{3}} \\
 &\times \sin \theta_{in} \frac{(\rho_p - \rho_0)}{(2\rho_p + \rho_0)} \left[1 + \frac{(\rho_p - \rho_0)}{(2\rho_p + \rho_0)} \left(\frac{R_p}{2h} \right)^3 + \frac{(\rho_p - \rho_0)^2}{(2\rho_p + \rho_0)^2} \left(\frac{R_p}{2h} \right)^6 \right] \left[1 + \left(\frac{R_p}{2h} \right)^3 \right] \\
 &\approx \frac{2}{3} k^2 R_p^3 (\mathbf{e}_r \cdot \mathbf{e}_{k_\perp}) \frac{(\rho_p - \rho_0)}{(2\rho_p + \rho_0)} \left[1 + \frac{3\rho_p}{(2\rho_p + \rho_0)} \left(\frac{R_p}{2h} \right)^3 + \frac{3\rho_p(\rho_p - \rho_0)}{(2\rho_p + \rho_0)^2} \left(\frac{R_p}{2h} \right)^6 \right]. \quad (32)
 \end{aligned}$$

In calculating the contribution of $\phi_1(\mathbf{r}')$, we used the fact that $a_{l-1} = -a_{l1}$, $\sin \theta' \cos \alpha' = \sqrt{2\pi/3} [Y_{l-1}^*(\theta', \alpha') - Y_{l1}^*(\theta', \alpha')]$, $\sin \theta' \sin \alpha' = i\sqrt{2\pi/3} [-Y_{l-1}^*(\theta', \alpha') - Y_{l1}^*(\theta', \alpha')]$. Summing up the contributions of individual terms, we obtain

$$\begin{aligned}
 f_2(\theta, \alpha) &= -\frac{2}{3} k^2 R_p^3 - \frac{2}{3} k^2 R_p^3 (\mathbf{e}_r \cdot \mathbf{e}_{k_\perp}) + \frac{2}{3} k^2 R_p^3 (\mathbf{e}_r \cdot \mathbf{e}_{k_\perp}) \\
 &+ \frac{4}{3} k^2 R_p^3 (\mathbf{e}_r \cdot \mathbf{e}_{k_\perp}) \frac{(\rho_p - \rho_0)}{(2\rho_p + \rho_0)} \left[1 - \frac{3\rho_0}{2(2\rho_p + \rho_0)} \left(\frac{R_p}{2h} \right)^3 - \frac{3\rho_0(\rho_p - \rho_0)}{2(2\rho_p + \rho_0)^2} \left(\frac{R_p}{2h} \right)^6 \right] \\
 &+ \frac{2}{3} k^2 R_p^3 (\mathbf{e}_r \cdot \mathbf{e}_{k_\perp}) \frac{(\rho_p - \rho_0)}{(2\rho_p + \rho_0)} \left[1 + \frac{3\rho_p}{(2\rho_p + \rho_0)} \left(\frac{R_p}{2h} \right)^3 + \frac{3\rho_p(\rho_p - \rho_0)}{(2\rho_p + \rho_0)^2} \left(\frac{R_p}{2h} \right)^6 \right] \\
 &= -\frac{2}{3} k^2 R_p^3 + 2k^2 R_p^3 (\mathbf{e}_r \cdot \mathbf{e}_{k_\perp}) \frac{(\rho_p - \rho_0)}{(2\rho_p + \rho_0)} \left[1 + \frac{(\rho_p - \rho_0)}{(2\rho_p + \rho_0)} \left(\frac{R_p}{2h} \right)^3 \right. \\
 &\quad \left. + \frac{(\rho_p - \rho_0)^2}{(2\rho_p + \rho_0)^2} \left(\frac{R_p}{2h} \right)^6 \right]. \quad (33)
 \end{aligned}$$

The given expression describes the contribution of the zeroth and first order terms to the scattering amplitude. However, a comparable contribution comes from second-order terms, which are not considered in this paper. This additional term is described by the following expression:

$$\Delta f_2 = \frac{(kR_p)^2}{4\pi\varphi_0} \int_{S_p} \frac{\partial}{\partial n'} [F_2(\mathbf{r}') + \Phi_2(\mathbf{r}')] dS'. \quad (34)$$

The integral in Eq. (34) describes the rate of change in particle volume. It does not depend on angles and the entire expression (34) describes the correction term to the monopole component of the scattering amplitude taking into account particle compressibility. A discussion of the effects associated with the manifestation of second-order terms is not given in this work due to the cumbersome nature of the corresponding calculations. However, an exception was made for Δf_2 due to the simplicity of the result:

$$\Delta f_2 = \frac{2}{3} (k^2 R_p^3) \frac{\rho_0 c_0^2}{\rho_p c_p^2}. \quad (35)$$

The scattering amplitude is determined by the contribution of the monopole and dipole sources. The reason why the monopole component of the scattering amplitude does not depend on the location of the particle relative to the boundary is as follows. The distance dependence is a manifestation of the interaction of the particle with the boundary. For a rigid boundary, this is equivalent to interaction with a mirror source. The interaction of a monopole source located at the center of a particle is carried out through disturbances in the surrounding incompressible liquid with divergence equal to zero. For this reason, the flux through the closed surface surrounding the imaginary source is zero. That is, disturbances do not affect the rate of change in the volume of the mirror source, which characterizes its monopole radiation. For this reason, interaction with a rigid boundary does not lead to a change in the monopole component of the scattering amplitude.

When the particle moves away from the surface $R_p/2h \rightarrow 0$, then the rescattering of the components reflected on the boundary can be neglected, and the sum of expressions (33) and (33) coincides with the double contribution to the scattering amplitude on a free particle from the monopole and dipole component associated with oscillations along the boundary. The factor 2 arises from the fact that the impenetrable boundary redistributes all radiation only to the upper half-space. The manuscript is supplied with Electronic Supplement, which contains plots describing dependence of the scattering amplitude on the observation angle and the distance to the boundary. This file also contains a comparison with the results of previously published works.

6. Discussion

The motion of particles in a fluid at the presence of acoustical field arises in applications that include the sorting, positioning, and levitation of such objects, as well as for ultrasonic cleaning. A new ultrasonic cleaning technique, the Ultrasonically Activated Stream (UAS),^{8,26–28} achieves cleaning with cold water streams through noninertial cavitation. If the bubbles are ultrasonically activated when they are on the target, the cleaning ability of the liquid is enhanced: the bubbles are attracted to the surface to be cleaned by Bjerknes radiation forces and are not as rapidly washed away by the flow as they would be in the absence of ultrasound.

Theoretical investigations of the acoustic radiation force acting on the active element - the bubble under the conditions of application of the UAS method were recently published.^{14,30} At the same time, the question remained open about the effect of the acoustic field on pollution particles, which, under the influence of micro-flows generated by bubbles, broke away from the wall and are carried away by the water flow. Wouldn't the presence of radiation force lead to adhesion of these particles to the surface being cleaned, only in a different place – downstream? The present study was an attempt to answer this question. For inorganic and organic pollutants, rigid and liquid sphere models were used, respectively.

Solving this problem in an approximation linear in the amplitude of the external field and finding the oscillatory flows in the vicinity of the inclusion makes it possible to compare their magnitude for the particle and the bubble. The conditions for implementing the UAM

method are as follows: bubbles and contamination particles 30 microns in size are in an ultrasonic field with a frequency of 135 kHz and the pressure amplitude of 50 kPa. For a particle located at a distance $h = 2R_p$ from the boundary at the same values of the material parameters that were used in constructing Fig. 2 and at the angle of incidence of $\theta_{in} = \pi/4$, Eq. (23) leads to the following displacement: $\Delta x \approx 0.3 \mu\text{m}$.

For a bubble, the dominant contribution to the displacement amplitude of surrounding liquid particles is made by radial pulsations.^{11,14} An estimate based on the same defining parameters leads to the following value of the amplitude of radial displacements $\Delta R \approx 8 \mu\text{m}$. Note, that for a resonant bubble with a radius $R_0 = 24 \mu\text{m}$, the difference can be even more significant.

The above estimate indicates the smallness of the radiation force exerted on the particle, since it is described by the quadratic form of the terms of the first approximation.^{15,20} Explicit expressions for the radiation force and comparisons with previously published results^{19,20} will be presented after taking into account second-order terms to describe the most commonly considered case of normal incidence.

The disadvantage of using a simplified – rigid boundary model can be corrected, since the existing difficulty in finding the long-wave expansion of the half-space Green’s function³¹ has been overcome.³²


7. Conclusions

A method is presented for obtaining an analytical expression for the Rayleigh scattering due to a sound wave incident on the fluid sphere near a planar rigid boundary. The method follows the approach of Dassios²² and extend previous findings.²¹ The effect of the interaction between the sphere and the boundary is strongest when the sphere is on the order of one sphere radius from the boundary. Comparison with numerical calculations confirms the validity of the obtained analytical expressions. The dominant disturbance arising in the long-wavelength approximation is dipole oscillations along the boundary surface.

Acknowledgments

This work was supported by the POI FEBRAS (project No. 121021700341-2).

ORCID

Alexey Maksimov  <https://orcid.org/0000-0002-6766-7972>

References

1. G. C. Gaunaurd and H. Huang, Acoustical scattering by a spherical object near a plane boundary, *J. Acoust. Soc. Am.* **96** (1996) 2526–2536.
2. G. C. Gaunaurd and H. Huang, Sound scattering by a spherical object near a hard flat bottom, *IEEE Transactions on Ultrasonics, Ferroelectrics, and Frequency Control.* **43** (1996) 690–700.

3. E. L. Shenderov, Diffraction of sound by an elastic or impedance sphere located near an impedance or elastic boundary of a half-space, *Acoust. Phys.* **48** (2002) 607–617.
4. N. S. Grigorieva, M. S. Kupriyanov, D. A. Mikhailova and D. B. Ostrovskiy, Sound wave scattering by a spherical scatterer located near an ice surface, *Acoust. Phys.* **62** (2016) 8–21.
5. N. S. Grigorieva, M. S. Kupriyanov, D. A. Stepanova, D. B. Ostrovskiy and I. A. Seleznev, Pulse scattering on an ice sphere submerged in a homogeneous waveguide covered with ice, *J. Theor. and Comput. Acoustics* **24** (2016) 1650014.
6. P. Zhang, H. Bachman, A. Ozcelik and T. G. Huang, Acoustic microfluidics, *Annual Review of Analytical Chemistry*. **13** (2020) 17–43.
7. J. Friend and L. Y. Yeo, Microscale acoustofluidics: Microfluidics driven via acoustics and ultrasonics, *Rev. Modern. Phys.* **83** (2011) 647–687.
8. P. R. Birkin, D. G. Offen and T. G. Leighton, An activated fluid stream – New techniques for cold water cleaning, *Ultrason. Sonochem.* **29** (2016) 612–618.
9. G. Dassios and R. Kleinman, *Low Frequency Scattering* (Oxford University Press, Oxford, 1999).
10. N. H. Oguz and A. Prosperetti, Bubble oscillations in the vicinity of a nearly plane free surface, *J. Acoust. Soc. Am.* **87** (1999) 2085–2092.
11. A. O. Maksimov, B. A. Burov, A. S. Salomatin and D. V. Chernykh, Sounds of marine seeps: A study of bubble activity near a rigid boundary, *J. Acoust. Soc. Am.* **136** (2014) 1065–1076.
12. A. B. Baynes and O. A. Godin, A semi-analytic, numerically efficient model for low-frequency sound scattering by an infinite cylinder located near a boundary, *J. Theor. and Comput. Acoustics* **28** (2020) 2050010.
13. A. O. Maksimov and Yu. A. Polovinka, Oscillations of a gas inclusion near an interface, *Acoust. Phys.* **63** (2017) 26–32.
14. A. O. Maksimov and Yu. A. Polovinka, Acoustic manifestations of a gas inclusion near an interface, *Acoust. Phys.* **64** (2018) 27–36.
15. L. P. Gor'kov, On the forces acting on a small particle in an acoustical field in an ideal fluid, *Sov. Phys. Dokl.* **6** (1962) 773–775.
16. T. S. Jerome, Yu. A. Ilinskii, E. A. Zabolotskaya and M. F. Hamilton, Born approximation of acoustic radiation force and torque on soft objects of arbitrary shape, *J. Acoust. Soc. Am.* **145** (2019) 36–44.
17. A. K. Miri and F. G. Miri, Acoustic radiation force on a spherical contrast agent shell near a vessel porous wall – Theory, *Ultrasound Med. Biol.* **37** (2011) 301–311.
18. Y. Zhang, W. Lin, C. Su and P. Wu, Axial acoustic radiation force on an elastic spherical shell near an impedance boundary for zero-order quasi-Bessel-Gauss beam, *Chin. Phys. B* **30** (2019) 044301.
19. T. Baasch and J. Dual, Acoustic radiation force on a spherical fluid or solid elastic particle placed close to a fluid or solid elastic half-space, *Phys. Rev. Appl.* **14** (2020) 024052.
20. B. E. Simon and M. F. Hamilton, Analytical solution for acoustic radiation force on a sphere near a planar boundary, *J. Acoust. Soc. Am.* **153** (2023) 627–642.
21. A. O. Maksimov, Peculiarities of Rayleigh scattering by a particle located near an interface, *Acoust. Phys.* **70** (2024) (In press).
22. G. Dassios and R. Kleinman, Half space scattering problems at low frequencies, *Journal of Applied Mathematics* **62** (1999) 61–79.
23. A. A. Doinikov and A. Bouakaz, Interaction of an ultrasound-activated contrast microbubble with a wall at arbitrary separation distances, *Phys. Med. Biol.* **60** (2015) 7909–7925.
24. R. J. A. Tough and A. J. Stone, Properties of the regular and irregular solid harmonics, *Journal of Physics A: Mathematical and General* **10** (1977) 1261–1269.
25. O. R. Gruzan, Translation addition theorems for spherical vector wave functions, *Quart. Appl. Math.* **20** (1962) 33–40.

26. M. Salta, L. R. Goodes, B. J. Maas, S. P. Dennington, T. J. Secker and T. G. Leighton, Bubbles versus biofilms: A novel method for the removal of marine biofilms attached on antifouling coatings using an ultrasonically activated water stream, *Surf. Topogr.: Metrol. Prop.* **4** (2016) 034009.
27. T. G. Secker, T. G. Leighton, D. G. Offin, P. R. Birkin, R. C. Herve and C. W. Keevil, A cold water, ultrasonically activated stream efficiently removes proteins and prion-associated amyloid from surgical stainless steel, *J. Hosp. Infect.* **106** (2020) 649–656.
28. M. Malakoutikhah, C. N. Dolder, T. J. Secker, M. Zhu, C. C. Harling, C. W. Keevil and T. G. Leighton, Industrial lubricant removal using an ultrasonically activated water stream, with potential application for coronavirus decontamination and infection prevention for SARS-CoV-2, *Trans. IMF Int. J. Surf. Eng. Coat.* **98** (2020) 258–270.
29. A. O. Maksimov and T. G. Leighton, Acoustic radiation force on a parametrically distorted bubble, *J. Acoust. Soc. Am.* **143** (2018) 296–305.
30. A. Maksimov, Radiation force on a bubble located near an interface, *J. Acoust. Soc. Am.* **151** (2022) 1464–1475.
31. A. R. Okoyenta, Haijun Wu, Xueliang Liu and Weikang Jiang, A short survey on Green’s function for acoustic problems, *J. Theor. and Comput. Acoustics* **28** (2020) 1950025.
32. A. Maksimov, Near field of the half-space Green’s function, *J. Theor. and Comput. Acoustics* **30** (2022) 2150019.